DALTON
FULL PAPER

Crystal structures of mixed-ligand oxocyano complexes of molybdenum(IV) and tungsten(IV) and their reactivity towards molecular oxygen studied by IR spectroscopy

Dariusz Matoga, Janusz Szklarzewicz, Alina Samotus * and Krzysztof Lewiński

Faculty of Chemistry, Jagiellonian University, R. Ingardena 3, 30-060 Kraków, Poland.
E-mail: Samotus@chemia.uj.edu.pl

Received 15th March 2002, Accepted 22nd July 2002
First published as an Advance Article on the web 27th August 2002

The series of compounds, $(PPh_4)_2[M(CN)_4O(L)]\cdot xH_2O$ [M = Mo, W; L = pyrazine (pz), pyridine (py); Ph = phenyl group; $x = 0, 2, 3$], $(PPh_4)_3[Mo(CN)_5O]\cdot 7H_2O$ and $K(PPh_4)_2[Mo(CN)_5O]\cdot 5H_2O$, which are able to bind molecular oxygen giving peroxo complexes $(PPh_4)_2[M(CN)_4O(O_2)]$, have been synthesised. The substrates were characterised by thermogravimetric analysis, vibrational and UV-VIS spectroscopy and the crystal structure determination of $(PPh_4)_2[M(CN)_4O(pz)]\cdot 3H_2O$. The latter salts are isomorphous and consist of anions of approximately octahedral geometry, forming a three-dimensional hydrogen-bonded network with channels that enable the penetration of dioxygen. The solid state reactions of all the salts with O_2 have been studied by measuring their infrared spectra. The integrated intensities of the O–O, pz or py, MO and C≡N bands change with time according to pseudo-first-order kinetics. The rate constants k_{obs} range from 0.37×10^{-4} to 1.04×10^{-4} s^{-1} at 323 K. A detailed study of the function of temperature has been undertaken for $(PPh_4)_2[W(CN)_4O(pz)]\cdot 3H_2O$. The activation parameters, $\Delta H^{\#} = 68 \pm 13$ kJ mol^{-1} and $\Delta S^{\#} = -117 \pm 39$ J K^{-1} mol^{-1}, were determined and an associative mechanism of dioxygen uptake was assumed.

Introduction

The reactions of transition metal complexes with molecular oxygen have been widely investigated for various metals,[1] *e.g.* Co, Fe, Mn, Cu, Ni, Ru, Rh, Pd, V, Cr, Ir, Mo, W, for over a hundred years. Such processes have been mainly studied in solution, but there are also reports on reactions carried out in the solid state,[2] especially with polymer and silica supported complexes.

It is characteristic that complexes of M(V) or M(VI) (M = Mo, W) have a tendency to react with H_2O_2 whereas those of M(IV) undergo reaction with molecular oxygen giving in both cases peroxo complexes.[3,4] In recent years the mixed-ligand tetracyanooxo complexes of molybdenum(IV) and tungsten(IV) of general formula $[M(CN)_4O(L)]^{n-}$, where L is a monodentate ligand such as CN^-, CH_3CN, pz (pyrazine), have been found useful in the activation of molecular oxygen.[5–8] In aerated polar organic solvents *e.g.* dichloromethane and acetonitrile they react with O_2 giving the same final product, $(PPh_4)_2[M(CN)_4O(O_2)]$ (Ph = phenyl group). The molybdenum complex has been structurally characterised[5,7] confirming the presence of a κ^2-peroxo ligand in *cis* position to the MoO bond. We have previously found that $(PPh_4)_2[M(CN)_4O(pz)]\cdot 3H_2O$, $(PPh_4)_3[W(CN)_5O]\cdot 7H_2O$ and $(PPh_4)_3[W(CN)_5O]$ reacted with dioxygen in the solid state[7,8] but a detailed study on the reaction kinetics was only done for $(PPh_4)_3[W(CN)_5O]$.[8]

In this work we have explored the use of molybdenum and tungsten oxocyano complexes as the solid substrates for reaction with molecular oxygen. We report here the crystal structures of two substrates that are the first structurally characterised examples of hydrated tetracyanooxo complexes of Mo and W with the ability to react with dioxygen. We have also studied the kinetics of the solid-state reactions with O_2 for all salts as well as the influence of various ligands, cation types, structural properties and the presence of water molecules on this process with the aim of facilitating the attachment of O_2 in the solid state.

Results and discussion

Characterisation of complexes

To study the influence of various factors on the solid-state reactions with dioxygen we have obtained a series of $[M(CN)_4O(L)]^{n-}$ type complexes (M = Mo or W) with different monodentate ligands L = pyrazine (pz), pyridine (py) or CN^-, using as cations either tetraphenylphosphonium ions alone (**1**–**3**, **6**–**9**, **11**) or the mixed cations: K^+ and PPh_4^+ (**4**), Cs^+ and Na^+ (**5**), K^+ and $[(CH_3)_4N]^+$ (**10**) (see the Experimental section for formulae details and numbering). We also compared the reactivity of hydrated (**6**, **11**) and anhydrous (**8**, **9**) salts.

The results of the thermogravimetric analyses are gathered in Table 1. They indicate that the dehydration of **1**, **3** and **11** takes place in two steps whereas in the other salts all of the water molecules are liberated in one step. The weight-loss measurements also show that the ligands L are released in the order: py > pz > CN^- and molybdenum complexes are slightly more stable than their tungsten analogues.

UV-VIS reflectance spectra have been measured for the molybdenum (**1**–**3**) and tungsten (**6**–**11**) salts. Each spectrum in the VIS/near UV part consists of a low-energy asymmetric band and a high-energy shoulder-like broad band. The second derivative analyses indicate that there are four bands in this region. The deconvolution of spectra into Gaussian curves gives the maxima which are listed in Table 2. The relatively low intensity of the four bands indicates that they correspond to spin-allowed d–d transitions, and their number is in agreement with the low symmetry of the complex anions (approximately C_{2v} for tetracyanides and C_{4v} for pentacyanides). The highest-energy d–d transition is taken as a measure of the ligand-field stabilization energy; it is biggest for **10**, which does not react with dioxygen.

In the UV region for all salts (excluding **10**) there are bands at approximately 273 and 237 nm corresponding to the tetraphenylphosphonium cation.[9] Additionally for pyrazine

DOI: 10.1039/b202654f

Table 1 Results of the thermogravimetric measurements

	Salt	T_{max}/K	Liberated molecules	Δm(%) Found (calc)	Decomposition temperature T/K
1	$(PPh_4)_2[Mo(CN)_4O(pz)]\cdot 3H_2O$	359	$2H_2O$	4.2 (3.5)	473
		388	$1H_2O$	1.8 (1.8)	
		428–458	pz	7.9 (7.8)	
2	$(PPh_4)_2[Mo(CN)_4O(py)]\cdot 2H_2O$	348	$2H_2O$	3.6 (3.6)	493
		358	py	6.6 (7.8)	
3	$(PPh_4)_3[Mo(CN)_5O]\cdot 7H_2O$	332	$5H_2O$	6.7 (6.5)	453
		368	$2H_2O$	1.9 (2.6)	
4	$K(PPh_4)_2[Mo(CN)_5O]\cdot 5H_2O$	338	$5H_2O$	9.1 (8.6)	453
6	$(PPh_4)_2[W(CN)_4O(pz)]\cdot 3H_2O$	378	$3H_2O$, pz	11.1 (12.0)	453
7	$(PPh_4)_2[W(CN)_4O(py)]\cdot 2H_2O$	330	$2H_2O$	3.2 (3.2)	463
		363	py	7.2 (7.2)	
11	$(PPh_4)_3[W(CN)_5O]\cdot 7H_2O^a$	328	$5H_2O$	–	433
		353	$2H_2O$	2.2 (2.4)	

^{a} Data obtained in the measurement with a heating rate of 5 K per minute (from ref. 6).

Table 2 Results of the second derivative analysis and deconvolution into Gaussian curves of the reflectance spectra

	Salt	Energy of d–d transitions E/cm^{-1} Gaussian deconvolution results
1	$(PPh_4)_2[Mo(CN)_4O(pz)]\cdot 3H_2O$	25800, 22820, 17070, 14660
2	$(PPh_4)_2[Mo(CN)_4O(py)]\cdot 2H_2O$	30410, 28520, 16830, 14670
3	$(PPh_4)_3[Mo(CN)_5O]\cdot 7H_2O$	25990, 23200, 16250, 13330
6	$(PPh_4)_2[W(CN)_4O(pz)]\cdot 3H_2O$	24750, 21770, 17840, 15510
7	$(PPh_4)_2[W(CN)_4O(py)]\cdot 2H_2O$	28590, 23410, 16380, 13130
8	$(PPh_4)_2[W(CN)_4O(pz)]$	24360, 20680, 16730, 14080
9	$(PPh_4)_3[W(CN)_5O]$	25380, 21230, 17760, 14510
10	$K(Me_4N)_2[W(CN)_5O]$	32860, 29570, 18300, 15370
11	$(PPh_4)_3[W(CN)_5O]\cdot 7H_2O$	24960, 21210, 16700, 14490

tetracyanides there is one more band in this region at about 310 nm which can be ascribed to the electronic transitions in pyrazine itself.[9] Pyridine also absorbs around 305 nm but its molar absorption coefficient is about 10 times smaller than that for pyrazine[10] and the band is not observed in the spectra.

Description of the structures of 1 and 6

Both salts, **1** and **6** were found to be isomorphous with only slightly different bond distances and angles. The crystal structure consists of $[M(CN)_4O(pz)]^{2-}$ anions, two tetraphenylphosphonium cations and three water molecules in the asymmetric part of the unit cell (Fig. 1). The structure comprises infinite chains of tetraphenylphosphonium cations propagating along the *a* direction which are stabilized by π stacking. They form two antiparallel strands of alternating face-to-face and face-to-edge geometry of interactions involving one phenyl ring of the first PPh_4^+ and two phenyl rings of the second cation. These chains are separated in the structure by layers of $[M(CN)_4O(pz)]^{2-}$ anions parallel to the (010) plane and layers parallel to the (001) plane occupied by water molecules. Pairs of tetracyanides related by a centre of symmetry are bonded through a network of hydrogen-bonds in which all of the water molecules are involved (Fig. 2). Water molecules play two distinct roles in the structure. Molecules O2 and O3 form a four-membered ring around a centre of symmetry and make hydrogen-bonds to cyano ligands of molecules from different layers. The third water molecule forms a bridge between one of the cyano ligands and a CH group of the pyrazine ring in the neighbouring anion. The position of this water molecule is close to the crossing of layers that separate chains of tetraphenylphosphonium cations and is not stabilised by strong hydrogen-bonds. The refinement of the crystal structure of **1** and **6** showed that multiple alternative positions for this O4 water molecule are possible. Two types of water molecules were also distinguished for **1** in the thermogravimetric measurement (Table 1).

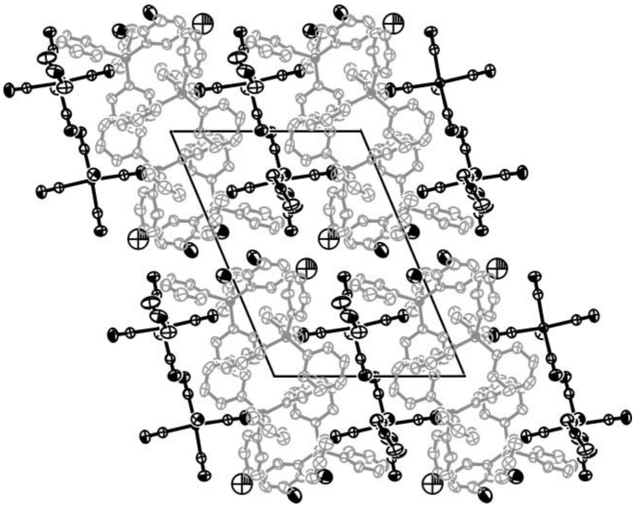

Fig. 1 Partial view of the structure of $(PPh_4)_2[W(CN)_4O(pz)]\cdot 3H_2O$ (**6**) along the *a* direction. H atoms are omitted for clarity.

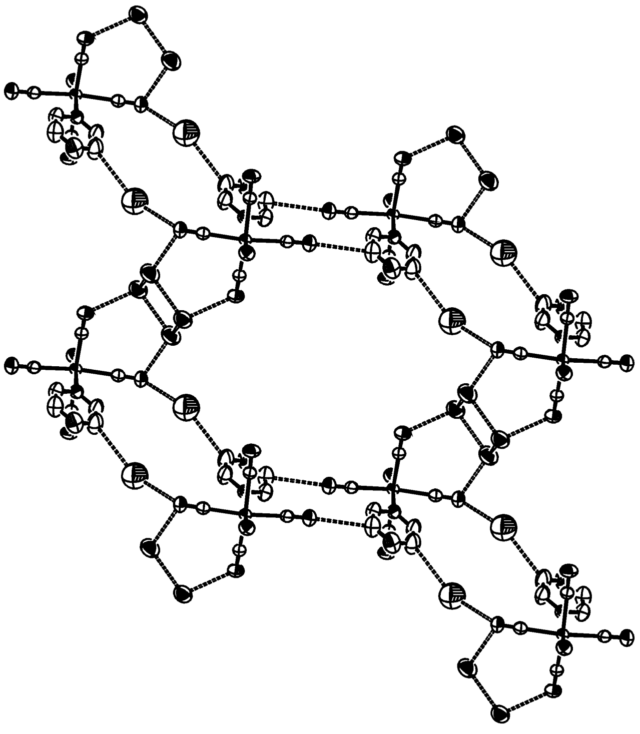

Fig. 2 Partial projection of the structure of $(PPh_4)_2[W(CN)_4O(pz)]\cdot 3H_2O$ (**6**) onto the (100) plane showing the hydrogen-bond network (dashed lines) connecting anions and water molecules.

The partial projection with the phenyl rings along the *a* direction (Fig. 1) permits the observation of the channel between two adjacent tetracyanides and the O4 water molecules. Such channels enable the penetration of molecular oxygen into the structures making the sites along them susceptible to attack by dioxygen.

The crystal structures of **1** and **6** showing the atomic numbering of the anions are represented by the example of **6** in Fig. 3.

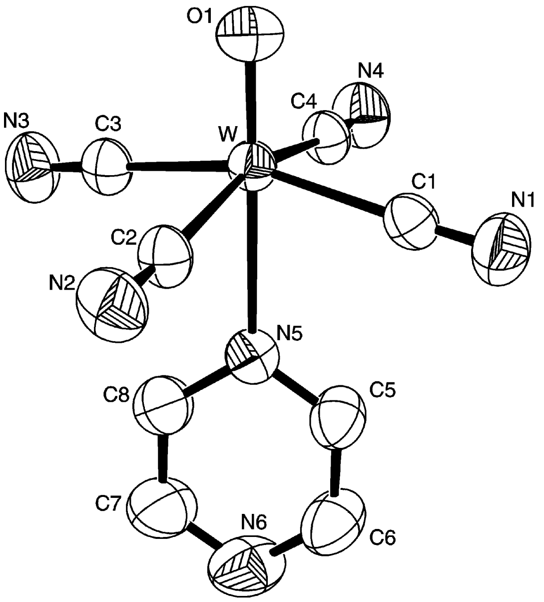

Fig. 3 Structure of the anion $[W(CN)_4O(pz)]^{2-}$ in the salt **6**, showing the atomic numbering. The atomic numbering in the anion of **1** is identical.

The complex anions exhibit distorted octahedral geometries and their symmetry is approximately C_{2v}.The oxo ligand and pyrazine occupy axial positions, and the four cyanides are equatorial. Central atoms are displaced towards the oxo ligand and the average O1–M–C angles are 100.0° for **1** and 99.9° for **6**. Selected bond lengths and angles are summarised in Table 3. The Mo–O1 bond distance in **1** (1.662 Å) is shorter than the corresponding bond in the tungsten salt (1.686 Å). All these bonds are relatively short and can be treated according to the classification of Cotton[11] as being almost triple ones (MO ≈ 1.65 Å). The M–C bond distances are almost the same within the structure for **6** and the average value is 2.144 Å whereas for **1** two pairs of M–C bond lengths are observed with averages of 2.156 Å and 2.170 Å. For the ligand in *trans* position to the M–O1 bond (pyrazine) the Mo–N5 distance in **1** is 2.569 Å and is longer than the W–N5 distance in **6** (2.521 Å). It is also the longest bond of this type yet observed among all the characterized tetracyanooxo complexes with monodentate ligands.[12]

Solid-state kinetics with molecular oxygen

We have found that all tetraphenylphosphonium salts **1**–**4**, **6**–**9**, **11** react in the solid state with dioxygen according to the overall stoichiometry illustrated by eqn. (1)–(3):

$$(PPh_4)_2[M^{IV}(CN)_4O(L)]\cdot xH_2O + O_2 \longrightarrow (PPh_4)_2[M^{VI}(CN)_4O(O_2)] + L + xH_2O \quad (1)$$

where L = pz or py; x = 0, 2 or 3

$$(PPh_4)_3[M^{IV}(CN)_5O]\cdot xH_2O + O_2 \longrightarrow (PPh_4)_2[M^{VI}(CN)_4O(O_2)] + (PPh_4)CN + xH_2O \quad (2)$$

where x = 0 or 7

$$K(PPh_4)_2[Mo^{IV}(CN)_5O]\cdot 5H_2O + O_2 \longrightarrow (PPh_4)_2[M^{VI}(CN)_4O(O_2)] + KCN + 5H_2O \quad (3)$$

Table 3 Selected bond lengths (Å) and angles (°) for $(PPh_4)_2[M(CN)_4O(pz)]\cdot 3H_2O$ (M = Mo **1**, M = W **6**) with estimated standard deviations in parentheses

	1 (M = Mo)	**6** (M = W)
M–O1	1.662(2)	1.686(2)
M–C1	2.156(3)	2.142(3)
M–C2	2.155(3)	2.148(3)
M–C3	2.171(3)	2.142(3)
M–C4	2.169(3)	2.144(3)
M–N5	2.569(3)	2.521(3)
C1–N1	1.137(4)	1.145(4)
C2–N2	1.144(4)	1.139(4)
C3–N3	1.139(4)	1.153(4)
C4–N4	1.132(4)	1.148(4)
N5–C5	1.325(4)	1.328(4)
N5–C8	1.333(5)	1.334(5)
C5–C6	1.396(6)	1.385(5)
N6–C6	1.295(6)	1.298(6)
N6–C7	1.316(6)	1.328(6)
C7–C8	1.381(6)	1.376(6)
O1–Mo–C1	99.66(12)	99.26(12)
O1–Mo–C2	99.13(12)	99.16(12)
O1–Mo–C3	100.68(12)	100.75(12)
O1–Mo–C4	100.59(12)	100.48(12)
O1–Mo–N5	175.65(10)	175.97(9)
C1–Mo–C2	89.78(11)	89.55(11)
C1–Mo–C3	159.61(12)	159.93(12)
C1–Mo–C4	88.10(11)	88.41(11)
C2–Mo–C3	88.44(11)	88.82(11)
C2–Mo–C4	160.25(12)	160.33(12)
C3–Mo–C4	86.76(11)	86.44(11)
N1–C1–Mo	177.9(3)	177.9(3)
N2–C2–Mo	176.6(3)	177.1(3)
N3–C3–Mo	179.7(4)	179.5(3)
N4–C4–Mo	173.7(3)	174.1(3)
N5–Mo–C1	79.51(10)	79.69(10)
N5–Mo–C2	76.63(10)	76.98(10)
N5–Mo–C3	80.32(10)	80.46(11)
N5–Mo–C4	83.68(10)	83.41(10)

Typical IR spectral changes occurring in air are exemplified for salt **6** in Fig. 4. They show the decrease in intensity of the substrate bands corresponding to metal–oxygen [$\nu_{max}(WO)_s$] vibrations at 969 cm^{-1} and those of the ligand in *trans* position to WO [ν_{max}(pz) at 1037 cm^{-1}], which is accompanied by an increase in intensity of the product bands ascribed to $(WO)_p$ at 933 cm^{-1} and O–O vibrations at 871 cm^{-1}, characteristic for $(PPh_4)_2[W(CN)_4O(O_2)]$.[7,8] While the reaction is proceeding the intensities of the C≡N bands of the substrates decrease which is typical for complexes with formal oxidation states V and VI. The C≡N signal in the product is very weak (see the inset in Fig. 4) and so is not observed in the spectra recorded for thin layers. During the reaction of salts **1**–**4**, **6**–**8** and **11** with dioxygen the integrated intensities of $(MO)_s$, $(MO)_p$, O–O, pz or py (L) and C≡N bands change with time according to pseudo-first-order kinetics. Their changes are exemplified for salt **6** in Fig. 5. The values of the pseudo-first-order rate constants, k_{obs} obtained from the exponential fits (eqn. (4)) are given in Table 4.

The rate constants of the hydrated molybdenum salts are similar with a tendency to decrease in the order L: py > pz > CN^-. In the case of the hydrated tungsten salts the order according to the decreasing value of k_{obs} is: pz > py. The salt with L = CN^- (**11**) undergoes dehydration at the measurement temperature and thus is not included in the tungsten series. The fastest incorporation of dioxygen occurs for **9** and the reaction proceeds two times faster for **6** than for **7** and **8** which have approximately the same rate constants (Table 4). The relatively weak dependence of rate constants on various leaving groups is favourable for an associative mechanism with dioxygen uptake as a rate-limiting step.

We have observed that dicaesium sodium pentacyanomolybdate(IV), **5** and bis(tetramethylammonium) potassium pentacyanooxotungstate(IV), **10** do not react with molecular oxygen.

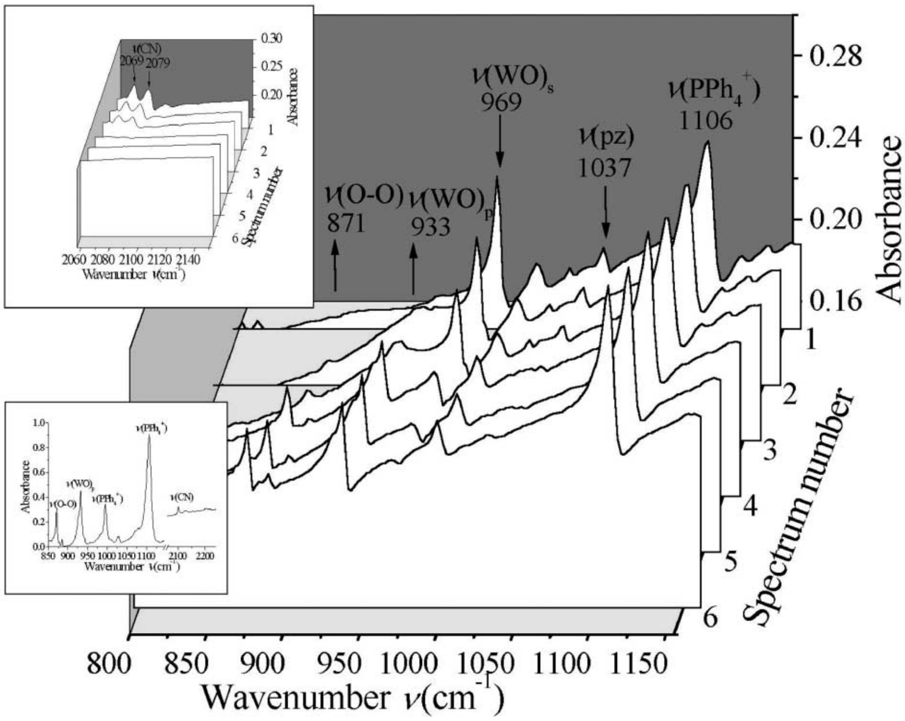

Fig. 4 The selected IR bands of $(PPh_4)_2[W(CN)_4O(pz)]\cdot3H_2O$ (**6**) kept in air at 313 K. Curve 1: initial spectrum. Curves 2–6: IR spectra recorded after 1 h 43 min, 3 h 43 min, 24 h 9 min, 45 h 56 min and 117 h 26 min of reaction with dioxygen, respectively. The inset in the top left corner presents the 2060–2150 cm^{-1} range. For comparison the IR spectrum of the product, $(PPh_4)_2[W(CN)_4O(O_2)]$ is given in the bottom left corner. Numbers indicate the band positions, ν/cm^{-1}.

Table 4 The kinetic data for the reaction with molecular oxygen in the solid state at 323 K monitored by the IR technique

	Salt	$k_{obs} \times 10^4$/s^{-1}
1	$(PPh_4)_2[Mo(CN)_4O(pz)]\cdot3H_2O$	0.54 ± 0.04
2	$(PPh_4)_2[Mo(CN)_4O(py)]\cdot2H_2O$	0.65 ± 0.08
3	$(PPh_4)_3[Mo(CN)_5O]\cdot7H_2O$	0.37 ± 0.09
4	$K(PPh_4)_2[Mo(CN)_5O]\cdot5H_2O$	0.48 ± 0.12
5	$Cs_2Na[Mo(CN)_5O]$	does not react
6	$(PPh_4)_2[W(CN)_4O(pz)]\cdot3H_2O$	1.04 ± 0.13
7	$(PPh_4)_2[W(CN)_4O(py)]\cdot2H_2O$	0.49 ± 0.08
8	$(PPh_4)_2[W(CN)_4O(pz)]$	0.45 ± 0.05 0.035 ± 0.016[a]
9	$(PPh_4)_3[W(CN)_5O]$	1.62 ± 0.24
10	$K(Me_4N)_2[W(CN)_5O]$	does not react

[a] Measured at 293 K.

Table 5 Kinetic data for the reaction of $(PPh_4)_2[W(CN)_4O(pz)]\cdot3H_2O$ (**6**) with molecular oxygen in the solid state

T/K	$k_{obs} \times 10^5$/s^{-1}	Thermodynamic parameters
295	0.20 ± 0.08	
301	0.80 ± 0.06	$\Delta H^{\#} = 68 \pm 13$ (kJ mol^{-1})
308	1.27 ± 0.12	$\Delta S^{\#} = -117 \pm 39$ (J K^{-1} mol^{-1})
313	1.7 ± 0.1	
317	3.1 ± 0.2	
320	3.0 ± 0.2	
323	10.4 ± 1.3	

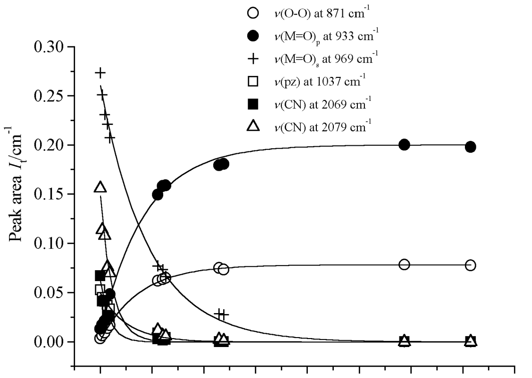

Fig. 5 The changes in the peak areas of selected bands in the IR spectrum of $(PPh_4)_2[W(CN)_4O(pz)]\cdot3H_2O$ (**6**), reacting in the solid state with molecular oxygen at 313 K, *versus* time.

We have also found that all salts with tetraphenylphosphonium cations as well as salt **4** with mixed cations, K^+ and PPh_4^+, are reactive towards O_2. These results indicate that the substrate for this reaction in the solid state needs a bulky aromatic cation, *e.g.* the tetraphenylphosphonium one. Such cations seem to form loose structures with channels that enable the penetration of dioxygen into the crystals as was found for **1** and **6**.

To study the influence of water molecules on the reaction rate, we have compared the kinetics of the pair of anhydrous **8** and hydrated **6** tungsten salts with pyrazine. At room temperature the rate constant is bigger for the anhydrous salt ($k_{obs} = 0.35 \times 10^{-5}$ s^{-1} at 293 K) than for hydrated one ($k_{obs} = 0.20 \times 10^{-5}$ s^{-1} at 295 K). At 323 K the opposite relation is observed (Tables 4 and 5). Thus, at room temperature the lack of water molecules facilitates the reaction. At higher temperatures, however, it seems that the rate for the anhydrous salt is limited by the diffusion of O_2 into the crystal. It may be due to structure collapse after dehydration (it proved to be irreversible for **6**) with decay of the channels used for the penetration of dioxygen. Reversible dehydration was previously reported[8] for salt **11** and the rate constant of its dehydrated salt **9** is the biggest of all the salts (Table 4). Thus, we suggest that dehydration favours the reaction with molecular oxygen unless it is accompanied by structural collapse. The collapse hinders the reaction with O_2 which can be particularly seen at higher temperatures when diffusion takes control over the process.

In the case of salt **6** the reaction with dioxygen was monitored at various temperatures and the values of the rate constants together with the thermodynamic parameters, $\Delta H^{\#}$ and $\Delta S^{\#}$, obtained by plotting $\ln(k_{obs}/T)$ *versus* $1/T$ (Fig. 6) and

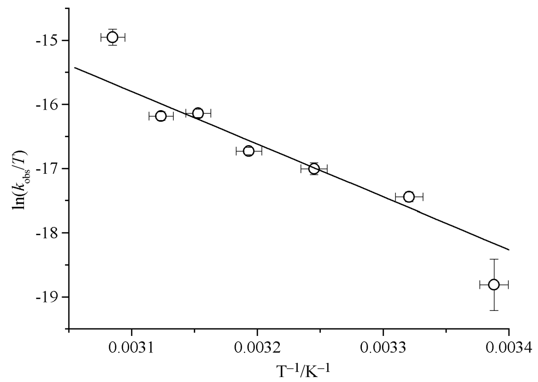

Fig. 6 The plot of $\ln(k_{obs}/T)$ *versus* $1/T$ for $(PPh_4)_2[W(CN)_4O(pz)]\cdot 3H_2O$ (**6**).

calculating the values of the slope and the intercept by linear regression, are summarised in Table 5. The negative value of the entropy of activation implies the associative mechanism of O_2 incorporation. Thus, the first stage of the reaction seems to involve nucleophilic attack of O_2 and electron transfer from M^{IV} to O_2, which is responsible for the rapid decrease in the intensity of the cyanide bands in all of the salts (Fig. 5). In the next step the ligand in *trans* position to the MO bond is released which is followed by rearrangement of the coordination sphere and the formation of a side-on peroxo ligand at the metal centre. However, the comparison of these data with solution kinetic measurements, carried out for $(PPh_4)_3[W(CN)_5O]\cdot 7H_2O$ reacting with O_2 in ethanol–acetone under pseudo-first-order conditions,[8] shows that the reaction may proceed according to the more complicated mechanism proposed for the reaction in solution.

Experimental

Starting materials and general procedures

The starting materials for the syntheses, $K_3Na[M(CN)_4O_2]\cdot 6H_2O$ (M = Mo, W) were prepared as described in the literature.[13,14] All ligands, other reagents and solvents were of analytical grade (Sigma-Aldrich or POCh) and used as supplied.

Carbon, hydrogen and nitrogen were determined by conventional organic microanalysis. UV-VIS absorption spectra were recorded on a Shimadzu UV 2101PC or on a Varian Cary 50 Conc spectrophotometers. Reflectance spectra were measured in $BaSO_4$ pellets *versus* $BaSO_4$ as reference (Shimadzu UV 2101PC with ISR-260 attachment). IR spectra were measured as KBr pellets on a Bruker IFS 48 spectrometer. Thermogravimetric analysis was performed on a Mettler thermoanalyser TGA/SDTA 851, under argon with a heating rate of 2 K per minute. The solid-state kinetics was studied by measuring IR spectra at 323 K (± 1 K) using NaCl plates covered with thin layers of the salts **1**–**10** which under these conditions transformed to the peroxo salts, $(PPh_4)_2[Mo(CN)_4O(O_2)]$ or $(PPh_4)_2[W(CN)_4O(O_2)]$. For salt **6** the monitoring was carried out additionally at 295, 301, 313, 317 and 320 K (± 1 K) and for salt **8** at 293 K. The spectra (measured in absorbance mode) were collected in time t and the integrated intensities I_t of the decreasing MO band ($(MO)_s$) of the substrate as well as the increase of both the O–O and MO ($(MO)_p$) bands of the product formed were taken for kinetic calculations for each salt. The strong band of PPh_4^+ at 1106 cm^{-1} was used as an internal intensity standard. The time dependence of I_t for each band i was fitted to eqn. (4).

$$I_t = I_\infty + (I_0 - I_\infty)\exp(-k_i t) \qquad (4)$$

The adjustable parameters were I_0, I_∞ and the pseudo-first-order rate constants, k_i. I_∞ is the integrated intensity at $t = \infty$ and I_0 is the integrated intensity at time $t = 0$. The final pseudo-first-order rate constants, k_{obs} for each salt were averaged over three values of k_i.

Syntheses

All salts: $(PPh_4)_2[Mo(CN)_4O(pz)]\cdot 3H_2O$ (**1**);[7] $Cs_2Na[Mo(CN)_5O]$ (**5**);[15] $(PPh_4)_2[W(CN)_4O(pz)]\cdot 3H_2O$ (**6**);[7] $(PPh_4)_3[W(CN)_5O]$ (**9**)[8] and $(PPh_4)_3[W(CN)_5O]\cdot 7H_2O$ (**11**)[8] were synthesised according to the methods described by us earlier. Their purity was confirmed by IR spectroscopy.

Bis(tetraphenylphosphonium) tetracyanooxopyridinemolybdate(IV) dihydrate, $(PPh_4)_2[Mo(CN)_4O(py)]\cdot 2H_2O$ (2). The anhydrous salt, $(PPh_4)_2[Mo(CN)_4O(py)]$ has been previously mentioned by Arzoumanian *et al.* as being obtained from $(PPh_4)_3[Mo(CN)_5O]$.[16] The salt **2** was prepared by dissolving $K_3Na[Mo(CN)_4O_2]\cdot 6H_2O$ (0.42 g, 0.87 mmol) in water (7 cm^3). The pH of the solution was adjusted to *ca.* 9.0 with HCl (3 M) and then pyridine (1 cm^3, 14.8 mmol) was added followed by $(PPh_4)Cl$ (0.75 g, 2 mmol). The resulting green crystals of **2** (0.37 g, 43%) were filtered off, washed two times with a small amount of water and dried in air (Found: C, 67.5; H, 4.9; N, 7.5. $C_{57}H_{49}MoN_5O_3P_2$ requires C, 67.8; H, 4.9; N, 6.9%); λ_{max}/nm (CH_2Cl_2 under N_2) 647 (ε_{max}/dm^3 mol^{-1} cm^{-1} 49); ν_{max}/cm^{-1} (MoO) 963vs and (CN) 2089m, 2098m and 2111vw (KBr). The salt is insoluble in water and acetone but soluble in such polar organic solvents as C_2H_5OH, CH_3CN and CH_2Cl_2.

Tris(tetraphenylphosphonium) pentacyanooxomolybdate(IV) heptahydrate, $(PPh_4)_3[Mo(CN)_5O]\cdot 7H_2O$ (3). We modified the method of synthesis described by Wieghardt *et al.*[17] using $Cs_2Na[Mo(CN)_5O]$ and KCN as starting materials. The reaction temperature was also lowered from 313 K to *ca.* 293 K. The salt **3** was prepared by dissolving $Cs_2Na[Mo(CN)_5O]$ (**5**) (0.16 g, 0.29 mmol) and KCN (0.42 g, 8.6 mmol) in water (10 cm^3). Then a solution of $(PPh_4)Cl$ (0.34 g, 0.91 mmol) in water (5 cm^3) was added. The mixture was left for two days at room temperature in air for crystallization. The resulting green crystals of **3** (0.3 g, 76%) were filtered off, washed several times with water and dried in air (Found: C, 66.3; H, 5.5; N, 5.0. $C_{77}H_{74}MoN_5O_8P_3$ requires C, 66.7; H, 5.4; N, 5.0%); ν_{max}/cm^{-1} (MoO) 933s and (CN) 2079s and 2102vw (KBr).

Bis(tetraphenylphosphonium) potassium pentacyanooxomolybdate(IV) pentahydrate, $K(PPh_4)_2[Mo(CN)_5O]\cdot 5H_2O$ (4). The salt was prepared by dissolving $K_3Na[Mo(CN)_4O_2]\cdot 6H_2O$ (0.5 g, 1 mmol) and KCN (0.1 g, 2 mmol) in water (10 cm^3). The pH of the solution was adjusted to *ca.* 9.0 with HCl (3 M) and then $(PPh_4)Cl$ (1.2 g, 3.2 mmol) was added. The resulting green crystals of **4** (0.56 g, 53%) were filtered off, washed several times with water and dried in air (Found: C, 61.3; H, 4.6; N, 6.5. $C_{53}H_{50}KMoN_5O_6P_2$ requires C, 60.6; H, 4.8; N, 6.7%); ν_{max}/cm^{-1} (MoO) 937s and (CN) 2079s, 2094vw and 2104vw (KBr).

Bis(tetraphenylphosphonium) tetracyanooxopyridinetungstate(IV) dihydrate, $(PPh_4)_2[W(CN)_4O(py)]\cdot 2H_2O$ (7). The salt was prepared by changing the proportions of substrates in the synthesis described by Roodt *et al.*[18] who obtained $(PPh_4)_2[W(CN)_4O(py)]\cdot 8H_2O$. The salt **7** was prepared by dissolving $K_3Na[W(CN)_4O_2]\cdot 6H_2O$ (0.34 g, 0.59 mmol) in water (7 cm^3). The pH of the solution was adjusted to *ca.* 7.0 with HCl (3 M) and then pyridine (1 cm^3, 14.8 mmol) was added followed by $(PPh_4)Cl$ (0.5 g, 1.47 mmol). The resulting green crystals of **7** (0.33 g, 51%) were filtered off, washed two times with a small amount of water and dried in air (Found: C, 62.4; H, 4.5; N, 6.5. $C_{57}H_{49}N_5O_3P_2W$ requires C, 62.4; H, 4.5; N, 6.4%); λ_{max}/nm (CH_2Cl_2 under N_2) 614 (ε_{max}/dm^3 mol^{-1} cm^{-1} 69); ν_{max}/cm^{-1} (WO) 960vs and (CN) 2076m and 2083m (KBr). The salt is insoluble in water and acetone but soluble in such polar organic solvents as C_2H_5OH, CH_3CN and CH_2Cl_2.

Table 6 Selected crystallographic data for $(PPh_4)_2[Mo(CN)_4O(pz)]\cdot3H_2O$ (**1**) and $(PPh_4)_2[W(CN)_4O(pz)]\cdot3H_2O$ (**6**)

	1	**6**
Empirical formula	$C_{56}H_{50}MoN_6O_4P_2$	$C_{56}H_{50}N_6O_4P_2W$
M	1028.90	1116.81
T/K	293(2)	293(2)
Crystal system	Triclinic	Triclinic
Space group	$P\bar{1}$	$P\bar{1}$
a/Å	13.5730(2)	13.6050(2)
b/Å	13.6890(2)	13.68400(10)
c/Å	16.9070(3)	16.8940(3)
α/°	69.3040(7)	69.2620(5)
β/°	89.2790(6)	89.2020(5)
γ/°	62.1020(6)	61.8950(5)
V/Å^3	2552.37(7)	2549.61(6)
Z	2	2
ρ_{calc}/Mg m^{-3}	1.339	1.455
μ/mm^{-1}	0.372	2.380
Reflections collected	20030	19887
Independent reflections	11650	11621
R_{int}	0.0212	0.0211
Goodness of fit on F^2	1.076	1.006
Final R indices [$I>2\sigma(I)$]		
$R1$	0.0506	0.0279
$wR2$	0.1355	0.0669

Bis(tetraphenylphosphonium) tetracyanooxopyridinetungstate(IV), $(PPh_4)_2[W(CN)_4O(pz)]$ (8). The anhydrous salt was obtained by dehydration of $(PPh_4)_2[W(CN)_4O(pz)]\cdot3H_2O$ (**6**) in a desiccator over P_4O_{10} under anaerobic conditions. After four days of dehydration a mass loss of 4.89% was observed which corresponds to the release of three water molecules (4.84%); ν_{max}/cm^{-1} (WO) 969vs and (CN) 2069m, 2078w and 2085vw (KBr).

Bis(tetramethylammonium) potassium pentacyanooxotungstate(IV), $K[(CH_3)_4N]_2[W(CN)_5O]$ (10). The salt was prepared by dissolving $K_3Na[W(CN)_4O_2]\cdot6H_2O$ (1.5 g, 2.64 mmol) and KCN (0.34 g, 5.22 mmol) in water (10 cm^3). The pH of the mixture was adjusted to *ca.* 8.7 with HCl (3 M) and then $[(CH_3)_4N]Br$ (1.4 g, 9.08 mmol) was added. The resulting blue precipitate of **10** (0.13 g, 11%) was filtered off, washed several times with ethanol and dried in air (Found: C, 30.1; H, 4.9; N, 18.4. $C_{13}H_{24}KN_7OW$ requires C, 30.2; H, 4.6; N, 19.0%); ν_{max}/cm^{-1} (WO) 935s and (CN) 2077vs and 2108vw (sh) (KBr). The salt is insoluble in C_2H_5OH, CH_3CN, acetone and CH_2Cl_2 but soluble in water.

X-Ray structure determination

Crystal data for these salts, and a summary of data collection and structure refinement parameters, are given in Table 6. The position of the Mo, W and P atoms was determined by Patterson methods; the remaining non-hydrogen atoms were located in successive difference Fourier syntheses. The hydrogen atoms of the pyrazine and phenyl rings were included in the structure factor calculations at idealised positions and were not refined. The hydrogen atoms of water molecule O2 were located from a difference Fourier map and included at fixed positions, and those of O3 and O4 could not be located. Water molecule O4 is positionally disordered with multiple alternative positions of low occupancy not included in the refinement. In the final refinement cycle all non-hydrogen atoms except for O4 were refined anisotropically. The largest peaks in the final difference maps were located near the Mo and W atoms. All calculations were performed using SHELXL; scattering factors and anomalous dispersion factors were those given in SHELXL.[19] The molecular structure drawings were made with the ORTEP-III program.[20]

CCDC reference numbers 181899 and 181900.

See http://www.rsc.org/suppdata/dt/b2/b202654f/ for crystallographic data in CIF or other electronic format.

Acknowledgements

This work was supported in part by the Polish Research Committee, KBN, Grant no. 3T09A 057 17.

References

1 (*a*) M. L. Tobe and J. Burgess, *Inorganic Reaction Mechanisms*, Addison-Wesley-Longman, Harlow, 1999, pp. 491, 544; (*b*) N. J. Henson, P. J. Hay and A. Redondo, *Inorg. Chem.*, 1999, **38**, 1618; (*c*) J. Tachibana, T. Fujihara, Y. Sasaki and T. Imamura, *Inorg. React. Mech. (Amsterdam)*, 2000, **2**, 85; (*d*) M. Kosugi, S. Hikichi, M. Akita and Y. Moro-oka, *J. Chem. Soc., Dalton Trans.*, 1999, 1369; (*e*) M. S. Reynolds and A. Butler, *Inorg. Chem.*, 1996, **35**, 2378.

2 (*a*) D. B. MacQueen, C. Lange, M. Calvin, J. W. Otvos, L. O. Spreer, C. B. Allan, A. Ganse and R. B. Frankel, *Inorg. Chim. Acta*, 1997, **263**, 125; (*b*) G. Q. Lim and R. Govind, *Inorg. Chim. Acta*, 1995, **230**, 219; (*c*) F. Goetz, K. Nakamoto and J. R. Ferraro, *J. Inorg. Nucl. Chem.*, 1977, **39**, 423.

3 M. H. Dickman and M. T. Pope, *Chem. Rev.*, 1994, **94**, 569.

4 T. Fujihara, K. Hoshiba, Y. Sasaki and T. Imamura, *Bull. Chem. Soc. Jpn.*, 2000, **73**, 383.

5 H. Arzoumanian, J. F. Petrignani, M. Pierrot, F. Ridouane and J. Sanchez, *Inorg. Chem.*, 1988, **27**, 3377.

6 H. Arzoumanian, M. Pierrot, F. Ridouane and J. Sanchez, *Transition Met. Chem.*, 1991, **16**, 422.

7 D. Matoga, J. Szklarzewicz, A. Samotus, J. Burgess, J. Fawcett and D. R. Russell, *Polyhedron*, 2000, **19**, 1503.

8 J. Szklarzewicz, D. Matoga, A. Samotus, J. Burgess, J. Fawcett and D. R. Russell, *Croat. Chim. Acta*, 2001, **74**, 529.

9 *UV Atlas of Organic Compounds*, Butterworth, London, 1966, vol. II.

10 *Catalogue Handbook of Fine Chemicals*, Aldrich, Poland, 1999–2000.

11 F. A. Cotton and R. M. Wing, *Inorg. Chem.*, 1965, **4**, 867.

12 A. Samotus, J. Szklarzewicz and D. Matoga, *Bull. Pol. Acad. Sci., Chem.*, 2002, **50**, 145, and refs. therein.

13 A. Samotus, M. Dudek and A. Kanas, *J. Inorg. Nucl. Chem.*, 1975, **37**, 943.

14 A. Roodt, S. S. Basson and J. G. Leipoldt, *Polyhedron*, 1994, **13**, 599.

15 M. Dudek and A. Samotus, *Transition Met. Chem.*, 1985, **10**, 271.

16 H. Arzoumanian, A. Bouraoui, V. Lazzeri, M. Rajzmann and H. Teruel, *New J. Chem.*, 1992, **16**, 965.

17 K. Wieghardt, G. Backes-Dahmann, W. Holzbach and W. J. Swiridoff, *Z. Anorg. Allg. Chem.*, 1983, **499**, 44.

18 A. Roodt, J. G. Leipoldt, S. S. Basson and I. M. Potgieter, *Transition Met. Chem.*, 1988, **13**, 336.

19 G. M. Sheldrick, SHELXL97, University of Göttingen, Germany, 1997.

20 M. N. Burnett and C. K. Johnson, ORTEP-III, Report ORNL-6895, Oak Ridge National Laboratory, TN, USA, 1996.